THE JOURNAL OF BIOLOGICAL CHEMISTRY
Vol. 276, No. 29, Issue of July 20, pp. 27415–27423, 2001

Printed in U.S.A.

Hagfish Hemoglobins

STRUCTURE, FUNCTION, AND OXYGEN-LINKED ASSOCIATION*

Received for publication, January 26, 2001, and in revised form, April 6, 2001
Published, JBC Papers in Press, April 9, 2001, DOI 10.1074/jbc.M100759200

Angela Fago‡, Laura Giangiacomo§, Rossana D'Avino¶, Vito Carratore¶, Mario Romano¶, Alberto Boffi§, and Emilia Chiancone§‖

From the ‡Department of Zoophysiology, University of Aarhus, Bldg. 131, Universitetsparken, DK 8000 Aarhus C, Denmark, the §Consiglio Nazionale delle Ricerche Center of Molecular Biology and Department of Biochemical Sciences, University "La Sapienza" P.le Aldo Moro 5, Roma 00185, Italy, and the ¶Consiglio Nazionale delle Ricerche Institute of Protein Biochemistry and Enzymology, Via Marconi 10, Napoli 80125, Italy

Cyclostomes, hagfishes and lampreys, contain hemoglobins that are monomeric when oxygenated and polymerize to dimers or tetramers when deoxygenated. The three major hemoglobin components (HbI, HbII, and HbIII) from the hagfish *Myxine glutinosa* have been characterized and compared with lamprey *Petromyzon marinus* HbV, whose x-ray crystal structure has been solved in the deoxygenated, dimeric state (Heaslet, H. A., and Royer, W. E., Jr. (1999) *Structure* 7, 517–526). Of these three, HbII bears the highest sequence similarity to *P. marinus* HbV. In HbI and HbIII the distal histidine is substituted by a glutamine residue and additional substitutions occur in residues located at the deoxy dimer interface of *P. marinus* HbV. Infrared spectroscopy of the CO derivatives, used to probe the distal pocket fine structure, brings out a correlation between the CO stretching frequencies and the rates of CO combination. Ultracentrifugation studies show that HbI and HbIII are monomeric in both the oxygenated and deoxygenated states under all conditions studied, whereas deoxy HbII forms dimers at acidic pH values, like *P. marinus* HbV. Accordingly, the oxygen affinities of HbI and HbIII are independent of pH, whereas HbII displays a Bohr effect below pH 7.2. HbII also forms heterodimers with HbIII and heterotetramers with HbI. The functional counterparts of heteropolymer formation are cooperativity in oxygen binding and the oxygen-linked binding of protons and bicarbonate. The observed effects are explained on the basis of the x-ray structure of *P. marinus* HbV and the association behavior of site-specific mutants (Qiu, Y., Maillett, D. H., Knapp, J., Olson, J. S., and Riggs, A. F. (2000) *J. Biol. Chem.* 275, 13517–13528).

In most vertebrate hemoglobins cooperativity in oxygen binding originates from the transition between a low affinity (T) and a high affinity (R) state of the familiar $\alpha_2\beta_2$ tetrameric molecule (1, 2). The structural constraints between unlike chains are such that isolated chains and $\alpha\beta$ dimers are devoid of cooperativity (3–5). In contrast, in invertebrate hemoglobins cooperativity in ligand binding may be present also within homodimeric molecules, as in HbI from the clam *Scapharca inaequivalvis* (6). In this hemoglobin cooperativity arises from the direct communication between the two heme groups through a subunit interface distinct from those of the vertebrate hemoglobin tetramer, because it is formed by the heme-carrying E and F helices (7).

A different mechanism of cooperativity in oxygen binding is operative in the hemoglobins from hagfishes and lampreys, the most primitive living chordates, often grouped together into the class of Agnatha (*jawless*) or Cyclostomata (*round-mouths*) (8). In these hemoglobins cooperative ligand binding is based on the existence of a finite equilibrium between high affinity monomers and low affinity oligomers, notably dimers and tetramers (9). The ligand-linked polymerization is responsible also for the Bohr effect (the decrease in oxygen affinity upon a decrease in pH). Despite these similarities, hagfishes and lampreys may have diverged before the separation between myoglobin and hemoglobin chains (10), a fact that may explain the differences in the functional properties of their hemoglobins, such as the lower cooperativity and Bohr effect which characterize the hagfish proteins (11). The structural basis for the decrease in oxygen affinity upon dimerization has been disclosed recently by the crystal structure of deoxygenated lamprey *Petromyzon marinus* HbV (12). The E helices and the AB corner form a novel subunit interface that stabilizes a dimeric assembly. The proximity of the heme groups to the interface and the displacement of the first part of the E helix that is coupled to dimer formation suggest that ligand affinity is affected directly by the disposition of distal residues.

The hemoglobins from hagfishes have been studied less extensively than those from lampreys, which are easier to catch because they migrate into freshwater rivers and streams to spawn rather than living most of the time burrowed in the sea bottom sand. A further difficulty that presumably hindered the elucidation of structure-function relationships in hagfish hemoglobins is the high multiplicity of components, which is due to genetic polymorphism (13–15).

A distinctive feature of hagfish hemoglobins concerns the oxygen-linked binding not only of protons but also of bicarbonate (16). Binding of bicarbonate to the hemoglobin favors transport of CO_2 as intracellular rather than plasma-dissolved bicarbonate, as generally observed in vertebrates, and at the same time favors oxygen unloading. In hagfish, bicarbonate produced by the intracellular hydration of CO_2 (catalyzed by carbonic anhydrase) is not transported to the plasma due to the absence of the anion-exchanger band III protein from the red blood cells membrane (17, 18). The molecular basis of the bicarbonate effect is not known. Interestingly, it is remarkably large in whole blood (19, 20) and in the hemolysate (15, 21) but

* This work was supported by the Danish Natural Research Council and by Ministero olella Università e Ricerca Scientifica e Tecnologica of Italy. The costs of publication of this article were defrayed in part by the payment of page charges. This article must therefore be hereby marked "*advertisement*" in accordance with 18 U.S.C. Section 1734 solely to indicate this fact.

‖ To whom correspondence should be addressed: Tel.: 39-6-494-0543; Fax: 39-6-444-0062; E-mail: emilia.chiancone@uniroma1.it.

is not present in the isolated hemoglobin components, suggesting that some form of interaction between them is required (21). In lamprey hemoglobins the oxygen-linked binding of bicarbonate does not occur (22).

The present work reports the structural and functional characterization of the three major hemoglobin components from the Atlantic hagfish *Myxine glutinosa*. Paleus *et al*. (23) isolated three hemoglobin fractions from this species. However, the high heterogeneity of their samples allowed the determination only of the primary structure of HbIII, the component characterized by the highest isoelectric point (24). To avoid the problems posed by hemoglobin multiplicity, in this work the individual hemolysates were analyzed by isoelectric focusing (15) and only those samples showing identical patterns with three distinct, common bands were pooled. At variance with the hemolysate, the oxygen affinity of the isolated hemoglobin components appeared at a first characterization to be essentially unaffected by pH and bicarbonate, a further indication that the molecular basis of these allosteric effects must reside in specific interactions between different components. Sedimentation velocity experiments carried out under conditions similar to those of the oxygen equilibrium experiments confirmed this contention and showed that the presence of HbII, the component characterized by an intermediate isoelectric point, is essential for oligomer formation. Possible structural reasons for these effects are proposed.

EXPERIMENTAL PROCEDURES

Hemolysate Preparation and Separation of the Hemoglobins—Specimen of *M. glutinosa* were captured in wooden traps placed on the sea bottom in the vicinity of Kristineberg Marine Biological Station (Fiskebackskil, Sweden) and transferred into tanks with running sea water. Blood was taken with heparinized syringes from the caudal sinus, as previously described (15). After plasma removal by low speed centrifugation, red blood cells from each individual were washed three times in cold 3.2% NaCl and frozen at −80 °C to facilitate hemolysis. A 3-fold volume of cold 10 mM HEPES buffer, pH 7.8, 0.5 mM EDTA was added to the thawed cells, and the hemolysate was centrifuged at 12,000 rpm for 20 min to eliminate cellular debris. Due to the high genetic polymorphism of hemoglobins in hagfishes (13–15), the individual hemolysates were analyzed for hemoglobin multiplicity by isoelectrofocusing on ultrathin (0.2 mm) 7.5% polyacrylamide gels using Ampholines in the pH range 3.5–10 (1/3) and 7–9 (2/3) on a Multiphore II system (Amersham Pharmacia Biotech) at 7 watts and 15 °C according to the instructions contained in the manual. After a 10-min prefocusing step, performed to avoid artifactual bands (15), a 1-μl sample was loaded on the alkaline region of the gel. More than 100 hemolysates were analyzed in this way. The number of bands detected in the samples varied from three to six. Only those samples (38 in total) showing the identical isoelectrophoretical pattern with the major three bands were pooled.

The hemolysate was stripped from organic phosphates and endogenous cofactors by passage through a Sephadex G-25 fine column equilibrated with 50 mM Tris buffer, pH 7.8, 0.1 M NaCl, and dialyzed against three changes of CO-equilibrated 10 mM Tris buffer, pH 7.8, before anion exchange chromatography. The three hemoglobins were separated on a DEAE-Sephacel column equilibrated with the same buffer and eluted with a 0–0.2 M NaCl gradient. The separated hemoglobin fractions were concentrated on 4-ml Ultrafree Millipore ultrafiltration tubes (cutoff 5000), dialyzed against three changes of CO-equilibrated 10 mM HEPES buffer, pH 7.8, 0.5 mM EDTA and stored in small aliquots at −80 °C. Under these conditions the samples remained stable for months. All preparative steps were performed at 0–4 °C.

Amino Acid Sequence Determination and Analysis—Heme was removed and the globin chains precipitated with acid acetone according to Rossi Fanelli *et al.* (25). The globin chains were purified by reverse-phase HPLC[1] on a Vydac C4 column (3.9 × 300 mm) by a 35–80% linear gradient of 50% acetonitrile (solvent B) in 40% acetonitrile, 0.1% trifluoroacetic acid (solvent A) over 20 min, at a flow rate of 1 ml/min. *S*-Pyridylethylation was performed according to Friedman *et al.* (26). The globin chains were submitted to digestion with endoproteinase Asp-N and to CNBr cleavage following the procedure described by Gross and Witkop (27). Peptides were separated in a Beckman System Gold apparatus by reverse-phase HPLC on a μ-Bondapak C18 column (3.9 × 300 mm) (Asp-N digest) and on an Aquapore RP-300 column (4.6 × 250 mm) (CNBr fragments) by mixing 0.1% trifluoroacetic acid (solvent A) and 0.08% trifluoroacetic acid in acetonitrile (solvent B) in a multistep linear gradient over 120 min, at a flow rate of 1 ml/min. Peaks were collected manually and dried in a Savant Speed Vac concentrator. Cleavage at the Asp-Pro bond was performed in HbII in 70% formic acid (28) directly on a Polybrene-coated filter, and partial deacylation of the blocked N terminus was achieved by treatment of the N-terminal Asp-N peptide with 30% trifluoroacetic acid for 2 h at 55 °C.

Automated repetitive Edman degradation was performed on a PerkinElmer Life Sciences Procise 492 sequencer. Mass spectrometry measurements were carried out on intact HbI and HbIII globins, on HbIIA and HbIIB *S*-pyridylethylated chains and on blocked N-terminal Asp-N peptides. Mass spectra were recorded in linear mode on a Voyager Elite matrix-assisted laser desorption time-of-flight mass spectrometer (PerSeptive, Framingham, MA). The protein samples were dissolved in 70% formic acid, and 0.5 μl of this solution was immediately applied using the sandwich method (29) in a 0.5-μl droplet of 0.1% trifluoroacetic acid on a target precoated with sinapinic acid followed by addition of further 0.5 μl of matrix solution. Mass determination was based on external calibration.

Multiple alignment of Agnatha globins was performed with ClustalW (30). The amino acid sequences used are *M. glutinosa* HbI and HbII, and the eight protein sequences are more similar to HbII based on a BLASTP search (31), namely *P. marinus* GLB5 (SWISS-Prot accession number P02208), GLB3 (P09968), and GLB1 (P09967); *Lampetra fluviatilis* GLB (P02207); *Mordacia mordax* GLB1 (P21197), GLB2 (P21198), and GLB3 (P21199); and *M. glutinosa* GLB3 (P02209).

Infrared Spectroscopy Measurements—FTIR spectra were measured on a MAGNA 760 Nicolet spectrometer equipped with an MCT detector. The protein solutions at a concentration of about 1 mM (heme) in 20 mM HEPES buffer, pH 7.0, were equilibrated with 1 atm of CO gas and a few microliters of a sodium dithionite solution were added (final concentration of about 10 mM). The spectra were measured at 20 °C in a CaF_2 cell with a 50-μm Teflon spacer; 512 scans at 2 cm^{-1} resolution were averaged. The spectra of the oxygenated proteins measured under the same experimental conditions (dithionite was omitted) were subtracted from the spectra of the CO derivative to obtain a flat baseline.

Analytical Ultracentrifugation Experiments—All experiments were carried out on a Beckman XL-A analytical ultracentrifuge, equipped with absorbance optics, and an An60-Ti rotor, at 10 °C. Sedimentation velocity experiments were performed at 40,000 rpm. Data were collected at an appropriate wavelength (555 or 540 nm for deoxy- and oxyhemoglobin, respectively) and at a spacing of 0.005 cm with three averages in a continuous scan mode. They were analyzed with the program DCDT, provided by Dr. Walter Stafford (Boston Biomedical Research Institute), which yields the sedimentation coefficients (32). The values were reconducted to water and 20 °C ($s_{20,w}$) using standard procedures. Sedimentation equilibrium experiments were carried out at 30,000, 35,000, and 40,000 rpm. Data were collected at a spacing of 0.001 cm with 10 averages in a step-scan mode every 3 h. Equilibrium was checked by comparing scans up to 24 h. Data sets were edited with REEDIT (J. Lary, National Analytical Ultracentrifugation Center, Storrs, CT) and fitted with NONLIN (PC version provided by Emory Braswell, National Analytical Ultracentrifugation Center) according to Johnson *et al.* (33). Data from different speeds were combined for global fitting. For fits to a monomer-dimer association scheme, the monomer molecular weight was fixed at the value determined from the amino acid sequence. The protein concentration varied in the range 20–250 μM (heme) in 200 mM HEPES buffer, pH 6.0 or 7.4, with or without 10 mM $NaHCO_3$; it was calculated from the spectra of the oxygenated derivatives using an extinction coefficient of 13.8 cm^{-1} mM^{-1} on a heme basis for the oxygenated derivative at 540 nm. To obtain the deoxygenated protein, the solution at the desired concentration was degassed in a stoppered vial with N_2. Cells were filled in an inflatable glove box (AtmosBag, Aldrich) after addition of sodium dithionite to avoid reoxygenation. As a control of the state of oxygenation, absorbance spectra of all samples were measured in the ultracentrifuge cell before and after the run.

Oxygen Equilibrium Experiments—Oxygen equilibria were measured at 10 °C in 100 mM HEPES buffer, at a concentration of 0.5 mM (heme) in the absence and presence of 4% CO_2, corresponding to a concentration of bicarbonate in solution of ~15 mM at pH 7.2 (34). Stepwise increases in oxygen saturation of 3-μl samples were obtained by a modified gas diffusion chamber connected to Wosthoff pumps for

[1] The abbreviations used are: HPLC, high performance liquid chromatography; FTIR, Fourier transform infrared; SW, sperm wale.

mixing pure N_2 with air, O_2, and CO_2 (35). The change in absorbance upon oxygenation was monitored at 436 nm. Oxygen affinity (p_{50}, the oxygen partial pressure necessary to achieve half-saturation) and cooperativity at half-saturation (n_{50}) were calculated from Hill plots (log $Y/(1 - Y)$ *versus* log pO_2, where Y is the fractional oxygen saturation). pH values of the hemoglobin solutions were measured by a thermostatted BMS Mk2 microelectrode connected to a PHM64 pH meter (Radiometer). In experiments performed in the presence of CO_2, pH values were measured after equilibration of the hemoglobin solutions with 4% CO_2 in thermostatted micro-tonometers (Radiometer). Oxygen binding experiments on the isolated hemoglobins were performed in the absence and presence of 0.1 M KCl or 4% CO_2 and 1 μM carbonic anhydrase. The functional interaction between different components was analyzed in hemoglobin mixtures at a 1:1 molar ratio, in the absence and presence of 4% CO_2 and 1 μM carbonic anhydrase.

Ligand Binding Kinetics—Kinetic measurements were carried out in an Applied Photophysics (Leatherhead, UK) rapid mixing apparatus on the isolated components. In the CO binding experiments, the protein solutions at a concentration of about 10 μM (heme) in 0.2 M HEPES buffer, pH 7.0, containing 10 mM sodium dithionite were mixed with the same buffer containing increasing amounts of dissolved CO gas. The reaction was followed at 434 nm (the absorbance maximum of the deoxy derivative) and at 20 °C. The second order rate constants were obtained from the pseudo first order plot by standard procedures. The O_2 dissociation experiments were carried out by mixing the oxygenated protein with a solution containing an excess (0.1 M) sodium dithionite under the same experimental conditions described for CO binding measurements.

RESULTS

Three hemoglobin fractions were separated from the *M. glutinosa* hemolysate by anion exchange chromatography and were named HbI, HbII, and HbIII in reverse order of elution to be consistent with the nomenclature adopted by Paleus *et al.* (23) based on increasing isoelectric points. These were assessed by isoelectrofocusing on polyacrylamide gels and correspond to 6.35, 7.35, and 8.90 for HbI, HbII, and HbIII, respectively (data not shown). The three hemoglobin fractions HbI, HbII, and HbIII occur in a ratio of ~15:50:35. Reverse phase HPLC and mass spectrometry show that each fraction separated on the DEAE-column contains essentially a single hemoglobin component, consistent with the fact that only the individual hemolysates presenting three major bands, common to all samples, were pooled. On reverse phase HPLC, HbI and HbIII elute as a single peak with average molecular masses of 17,033 and 16,643, respectively, whereas HbII resolves into two single, separate peaks, named HbII A and HbII B, with molecular masses of 17,790 and 17,993, respectively (data not shown). The molecular mass and the N-terminal sequence of the first five residues indicated that HbIII corresponds to the component (SWISS-PROT accession number P02209) sequenced by Liljeqvist *et al.* (24).

The complete amino acid sequences of HbI and of HbII A and B were obtained by automated repetitive Edman degradation of the intact chain, of the HPLC purified Asp-N and CNBr peptides, and of the HbII fragment generated after cleavage of the single Asp-Pro bond.

Sequence of HbI—Direct sequencing of the intact chain proceeded to Glu-40 and provided the overlaps between the first three Asp-N peptides (N1-N2-N3) as shown in Fig. 1. Incomplete cleavage at Asp residues 65 and 87 yielded peptide N4-N6, whose sequence proceeded from residues 49 to 89, providing the overlap of peptides N4, N5, and N6-N7. The expected N7 peptide, comprising residues 112–146, was not recovered, indicating that Asp-N endoproteinase failed to cleave at Asp-112. The resulting N6-N7 peptide coeluted with an N4-N5 uncleaved peptide and its sequence (up to Phe-121) was obtained unambiguously by subtracting the sequences of the N4 and N5 peptides. The lack of any detectable sequence after acidic treatment indicated the absence of the single Asp-Pro bond characteristic of globin chains. The sequence from Phe-121 to Tyr-146 was obtained from the CNBr fragments, which also provided the necessary overlaps to the Asp-N peptides. CNBr cleavage yielded three peptides. CB2 provided the sequence from Lys-93 to Met-113 and CB3 the sequence from Phe-114 to Glu-148. CB1 corresponds to the N-terminal part of the chain (residues 1–92).

The complete amino acid sequence of HbI consists of 148 residues (Fig. 1). The calculated molecular weight of HbI is 17,027, in agreement with the value of 17,033 measured by mass spectrometry.

Sequence of HbII A and B—The Edman degradation of the intact chain was unsuccessful due to the presence of a blocking group at the N terminus. This was established to be an acetyl group by mass spectrometry measurements. The sequence of the N-terminal peptide N1 was obtained after deacylation of the N-terminal Ser as described under "Experimental Procedures."

Following Asp-Pro cleavage, the internal sequences from Pro-111 to Ser-138 for HbII A and from Pro-111 to Glu-135 for HbII B were obtained (Fig. 1). The two sequences are identical except for residue 134, which is Gly in HbII A and Ala in HbII B. The Asp-N peptides of the two globins were purified in a single HPLC chromatography run using identical conditions. Comparison of the elution patterns indicated that all the peaks have the same elution time except those corresponding to peptides N6 and N10. The sequence was determined for all the peaks of HbII B and for peptides N6 and N10 of HbII A. The two N6 and N10 peptides of HbII A differed from the corresponding peptides of HbII B at only one position, namely 83 (N6) and 134 (N10) with Ile and Gly, respectively, in HbII A, and Thr and Ala, respectively, in HbII B, in agreement with the molecular masses measured by mass spectrometry. The sequence of peptides N9 and N10, coeluting in the same peak, were unambiguously established, because the fragment corresponding to N10 was also recovered as two distinct peptides, named E1 and E2 (see Fig. 1), originating from an additional cleavage at Glu-135. The CNBr fragments and partially uncleaved Asp-N peptides provided the complete overlap of all the Asp-N peptides.

The complete amino acid sequence of HbII comprises 155 residues (Fig. 1). The calculated molecular mass is 17,690 for HbII A and 17,692 for HbII B. These values are in good agreement with those obtained by mass spectrometry of the *S*-pyridylethylated chains (17,791 and 17,794, respectively) after subtracting the mass of the pyridylethyl group at Cys-149.

Sequence Analysis—The sequences of *M. glutinosa* HbI, HbII, and HbIII (24) were compared with those of the lampreys *Lampetra fluviatilis*, *P. marinus*, and *Mordacia mordax* in an alignment made with ClustalW. In Fig. 2, only the sequence of *P. marinus* HbV is shown as representative of all lamprey hemoglobins for the sake of simplicity. *M. glutinosa* HbII is the only known cyclostome hemoglobin with a blocked N terminus. Moreover, it lacks the first three residues and has two insertions relative to the other hemoglobins, one of a single residue at the FG corner, the other of eight residues in the region corresponding to the GH corner in vertebrate globins. HbI and HbIII lack one residue at the GH corner and two residues at the CD corner, and have a two-residue extension at the C terminus relative to HbII and to lamprey hemoglobins. Interestingly, HbI and HbIII possess a glutamine residue in the distal position E7 instead of the canonical distal histidine.

Infrared Spectroscopy of the Isolated Hemoglobins—To gain information on structural features of the distal pocket that are relevant for ligand binding, infrared spectra were measured in the region of the stretching frequency of the bound CO molecule (2000–1900 cm^{-1}). The three main hemoglobin components have distinct absorption peaks (Fig. 3). HbI-CO has an absorption line at 1942 cm^{-1}, HbII-CO is characterized by a sharp

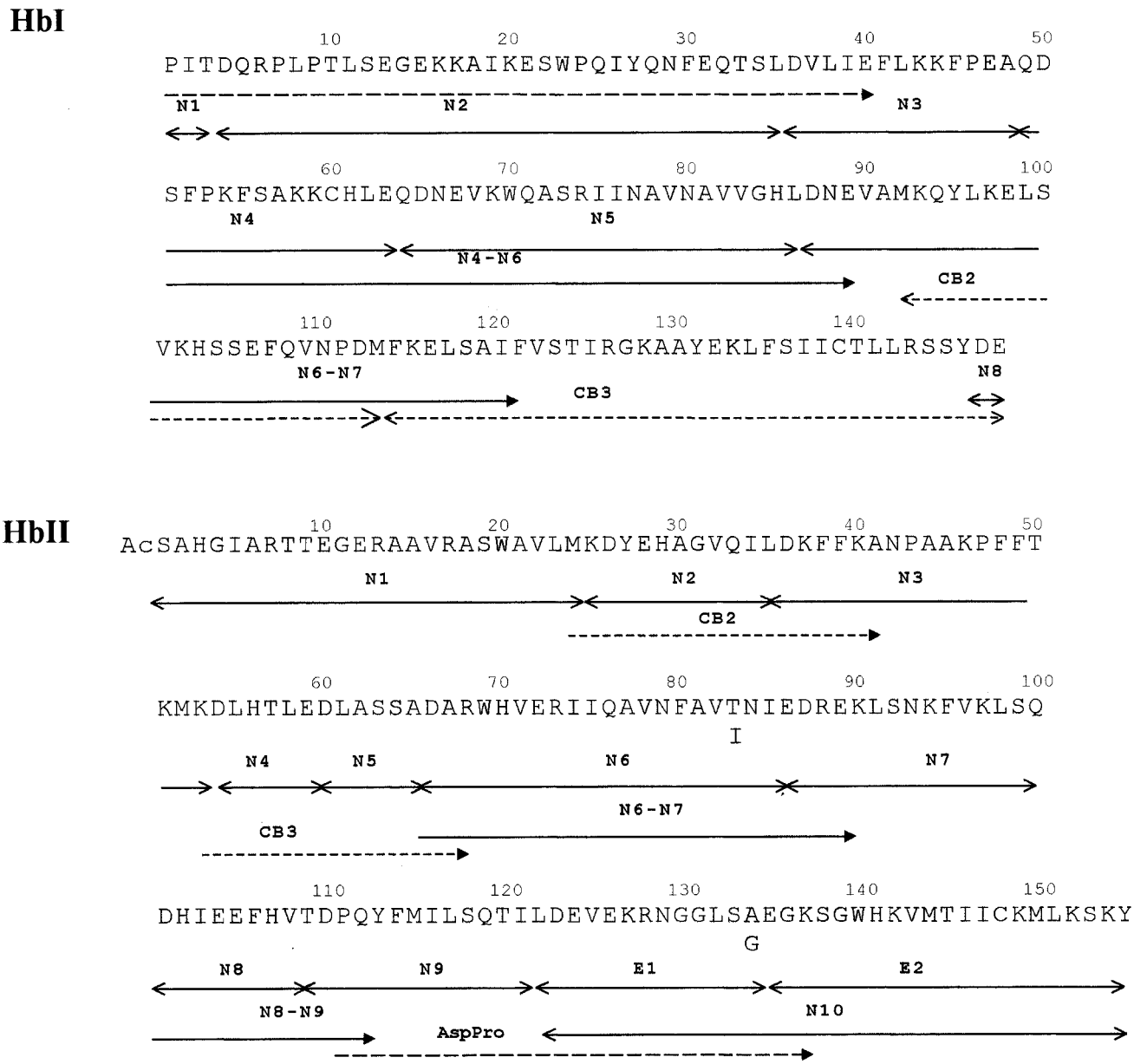

FIG. 1. **Amino acid sequence of *M. glutinosa* HbI (*top*) and HbII (*bottom*).** The various fragments used to reconstruct the sequence are shown. *Dashed arrows* indicate the residues identified by direct automated Edman degradation of the intact protein. *N*, peptides obtained by digestion with endoproteinase Asp-N; *CB*, cyanogen bromide peptides; *AspPro*, Asp-Pro cleavage peptides.

absorption peak at 1968 cm^{-1}, whereas HbIII-CO displays a broad and asymmetric absorption band centered at 1942 cm^{-1}. The spectrum of the hemolysate is included in Fig. 3; it appears to be dominated by the contributions of the most abundant components, HbII and HbIII.

Functional Properties of the Isolated Hemoglobins—The results of oxygen equilibrium experiments are presented in Fig. 4. The isolated hemoglobins bind oxygen with no cooperativity (Hill coefficient, n_{50}, around unity) and with an affinity that is virtually independent on pH and on the presence of bicarbonate or KCl (data not shown). Only HbII displays a slight Bohr effect below pH 7.2 (Bohr factor, $\Delta \log p_{50}/\Delta \log pH = -0.48$ at pH 7.0) both in the absence and in the presence of bicarbonate. HbIII is characterized by a lower oxygen affinity than HbII and HbI in having an about 2-fold higher p_{50} value.

The rates of oxygen dissociation from the three components are in accordance with the oxygen equilibrium measurements, because they parallel the values of p_{50} as in all myoglobins and hemoglobins (36). Thus, the rate of oxygen release decreases in the order HbIII, HbII, and HbI (Table I). In contrast, the second order rates of CO binding follow a different trend. CO binds about 8-fold faster to HbII than to HbI and HbIII, as indicated in the same table. Both reactions are independent of pH in the range 6.2–9.0 (data not shown).

Oxygen-linked Interactions between the Hemoglobins—The occurrence of oxygen-linked interactions between the different hemoglobin components was studied in the equimolar binary mixtures HbI+HbII, HbII+HbIII, and HbI+HbIII (Fig. 5). When HbI and HbII are present in solution at the same concentration, a distinct increase in the values of p_{50} and cooperativity is observed relative to the isolated components. Concomitantly, marked effects of pH (the Bohr factor is −0.50) and CO_2 become apparent, indicating oxygen-linked binding of protons and bicarbonate anions. A similar Bohr effect, but only in the presence of CO_2, is observed in the mixture HbII+HbIII. Under these conditions the p_{50} value increases relative to the

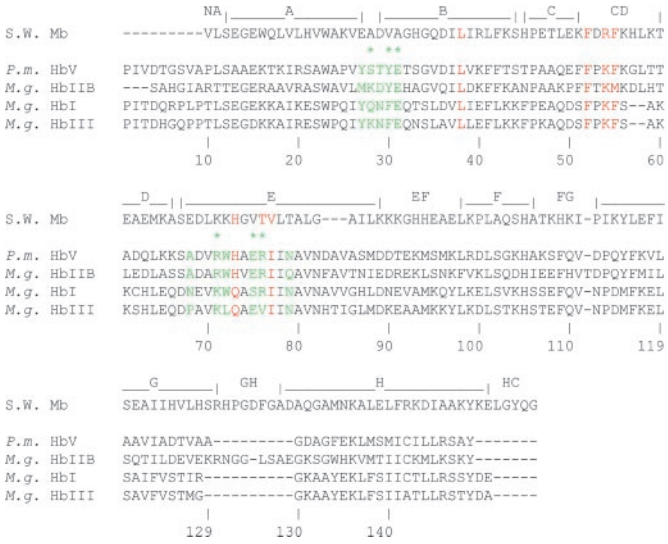

FIG. 2. **Amino acid sequence alignment of *M. glutinosa* hemoglobins with *Physeter catodon* myoglobin (*S.W. Mb*) and *Petromyzon marinus* HbV.** The *helix notation* refers to sperm whale myoglobin, the *numbering* refers to *P. marinus* HbV. Residues in the distal heme pocket are in *red*; residues at the dimer interface in *P. marinus* HbV are in *green*, those involved in the hydrogen bonding network at this interface are marked with an *asterisk*.

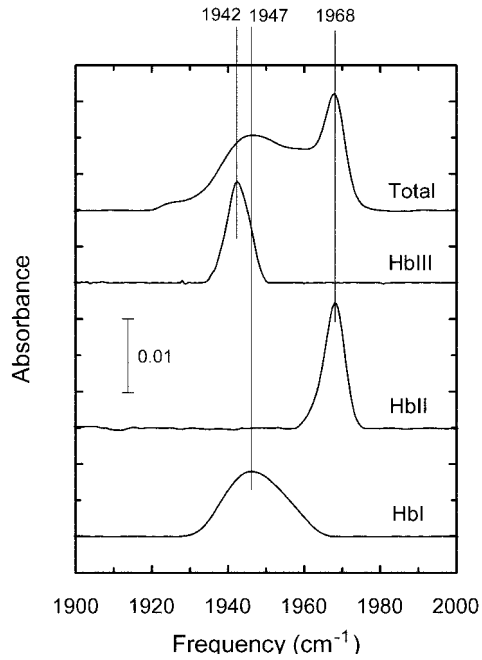

FIG. 3. **FTIR absorption spectra of *M. glutinosa* hemoglobins in the CO stretching region.** Protein concentration was 1.4–1.6 mM (heme). The hemolysate (total) was about 2 mM heme. All spectra were measured in 200 mM HEPES buffer at pH 7.0 and 20 °C in a 50-μm CaF_2 cell.

isolated components, but the effect is less marked than in the HbI+HbII mixture. In contrast, HbI and HbIII do not show any functional interaction as the oxygen binding properties of the mixture correspond to the average of those of the individual components.

The existence of association-dissociation equilibria as the structural basis of the functional interactions operative in the hemoglobin mixtures was assessed in sedimentation velocity experiments. These were conducted on the single components as a control, on their equimolar binary mixtures as well as on the hemolysate. The measurements were carried out on both the oxygenated and deoxygenated derivatives at two pH values, namely 6.0 and 7.4, in the absence and in the presence of 10 mM $NaHCO_3$.

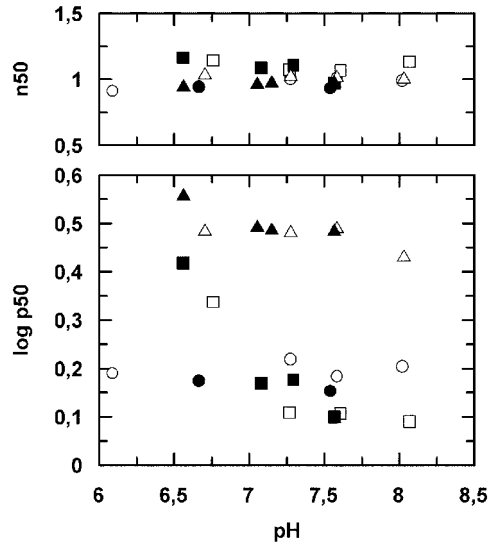

FIG. 4. **Oxygen equilibria of isolated *M. glutinosa* hemoglobins as a function of pH.** The temperature was 10 °C. The protein concentration was 0.5 mM (heme) in 100 mM HEPES buffer with (*full symbols*) or without (*empty symbols*) 10 mM $NaHCO_3$. HbI (*circles*); HbII (*squares*); HbIII (*triangles*).

TABLE I
Kinetics of CO binding and oxygen dissociation from HbI, HbII, and HbIII hemoglobins from M. glutinosa

All experiments were carried out in 200 mM HEPES buffer at pH 7.0 and 20 °C.

Protein	k_{CO}	k_{O2}
	$\mu M^{-1}\ s^{-1}$	s^{-1}
HbI	0.16 ± 0.2	61 ± 3
HbII	1.1 ± 0.1	82 ± 4
HbIII	0.13 ± 0.4	146 ± 8

In the liganded form the individual *M. glutinosa* hemoglobins and their binary mixtures sediment as monomers ($s_{20,w}$ 1.5–1.8 S) under all experimental conditions examined. The addition of bicarbonate has no effect on the state of association. In the deoxygenated form, the individual hemoglobins likewise sediment as monomers, with the exception of HbII at pH values below 7.2 where a single peak with $s_{20,w}$ of about 2.1 S, indicative of dimer formation, is observed. On the basis of this result, sedimentation equilibrium experiments were performed at pH 6.0 and 10 °C; they yielded a dimerization equilibrium constant $K_{1,2}$ of 450 ± 60 and 170 ± 10 M^{-1} in the absence and presence of 10 mM bicarbonate, respectively (Fig. 6).

In the deoxygenated form, the HbI+HbII mixtures polymerize at pH 6.0 and 7.4 both in the absence and in the presence of bicarbonate. Single peaks are observed whose $s_{20,w}$ values, 3.5–3.8 and 4.1 *S*, respectively, are intermediate between those of hemoglobin dimers (2.8 S) and tetramers (4.5 S), an indication that both oligomers are formed. In the deoxygenated HbII+HbIII mixtures at pH 6.0 the sedimentation coefficient increases from 1.8 to 2.6 S when bicarbonate is present, indicating that under these conditions dimerization occurs. In contrast, no polymerization can be detected at pH 7.4 both in the absence and in the presence of bicarbonate. The HbI+HbIII mixtures do not show polymerization when deoxygenated. The experimentally determined sedimentation coefficients are summarized in Table II; representative sedimentation patterns are presented in Fig. 7.

The sedimentation velocity experiments conducted on the hemolysate at pH 7.4 are consistent with the data on the single

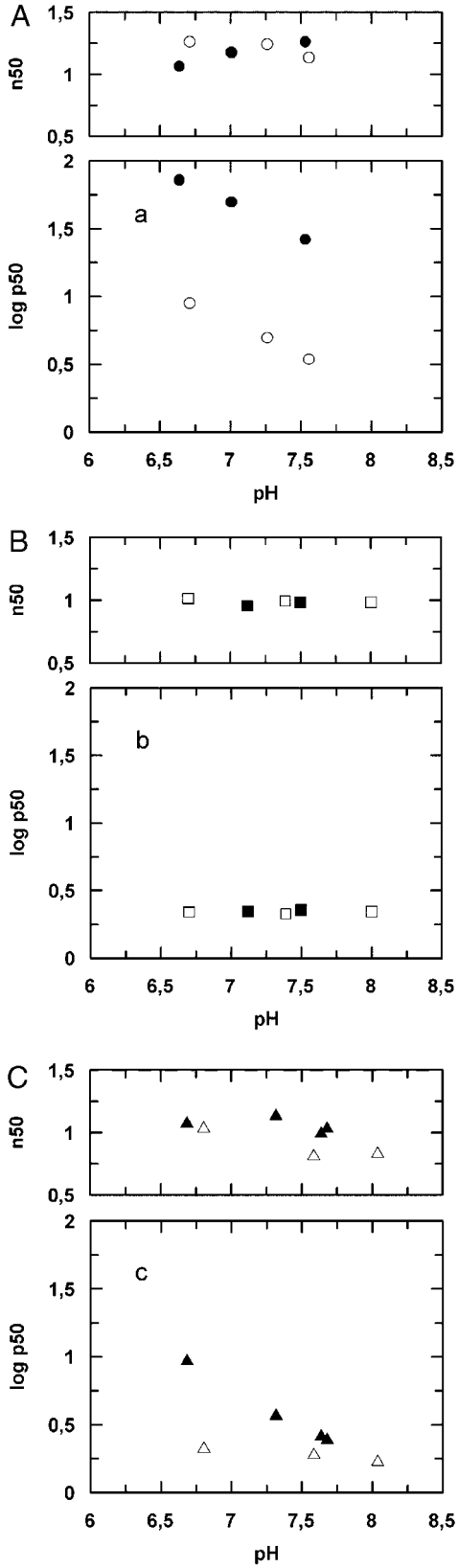

FIG. 5. **Oxygen equilibria of binary equimolar mixtures of *M. glutinosa* hemoglobins.** The temperature was 10 °C. The protein concentration was 0.5 mM (heme) in 100 mM HEPES buffer with (*full symbols*) or without (*empty symbols*) 10 mM $NaHCO_3$. *a*, HbI+HbII; *b*, HbI+HbIII; *c*, HbII+HbIII.

components and on their equimolar binary mixtures. Thus, in the presence of oxygen, the hemolysate sediments as a single homogeneous peak with $s_{20,w}$ of about 1.8 S. Upon deoxygenation, in accordance with previous gel filtration data (16), a monomer ($s_{20,w}$ ~ 1.7 S) and an oligomer peak ($s_{20,w}$ ~ 4.1 S) can be detected (Fig. 7*d*). The amount of tetramers formed is around 30% as expected on the basis of the hemolysate composition (15% HbI, 50% HbII, 35% HbIII) and of the fact that at pH 7.4 only HbI and HbII are able to polymerize giving rise to heterotetramers (Table II).

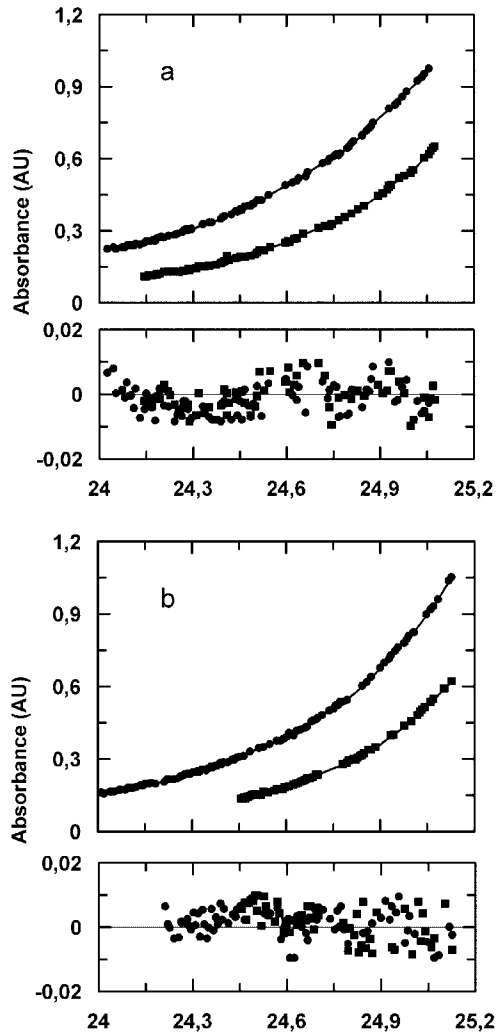

FIG. 6. **Sedimentation equilibrium of deoxygenated HbII.** The experiments were conducted at 10 °C and 30,000 (*circles*) or 35,000 (*squares*) rpm. The protein concentration was 250 μM (heme) in 200 mM HEPES buffer pH 6.0 in the absence (*a*) or in the presence (*b*) of 10 mM $NaHCO_3$. The data are fitted to a monomer-dimer model. Residuals are shown in the *lower panels*.

DISCUSSION

The present study of the three major hemoglobins from the hagfish *M. glutinosa* provides the basis for understanding the complex oxygen-linked phenomena that take place in the hemolysate and the distinctive differences relative to lamprey hemoglobins. First, the *M. glutinosa* hemoglobins have been investigated separately to assess their structural and intrinsic ligand binding properties. Thereafter, binary mixtures have been analyzed to establish the role played by each component in oxygen-linked polymer formation.

The sequences of HbI, HbII, and HbIII presented in Fig. 2 bring out the high overall similarity with *P. marinus* HbV. They also indicate that in the *M. glutinosa* hemoglobins the heme pocket geometry is superimposable to that of sperm whale (SW) myoglobin. However, there are substitutions in key positions of the distal pocket, namely: (i) a glutamine residue

TABLE II
Sedimentation coefficients of binary equimolar mixtures of M. glutinosa hemoglobins in the deoxygenated state

Sedimentation coefficients, $s_{20,w}$, in Svedbergs. Protein concentration was 150 μM (heme) in 200 mM HEPES buffer pH 6.0 or 7.4 with or without 10 mM $NaHCO_3$.

$NaHCO_3$	HbI+HbII		HbII+HbIII	
	−	+	−	+
pH		*S*		
6.0	3.49		1.78	2.57
7.4	3.85	4.15	1.48	1.99

instead of the canonical distal histidine in position E7 in both HbI and HbIII; (ii) a valine residue in position E10 in HbIII (Thr in SW-Mb and Arg in lamprey and in the other two hagfish components); (iii) a methionine residue at position CD4 in HbII instead of phenylalanine in SW-Mb and in the other hemoglobins considered.

The fine structure of the distal pocket has been probed by measuring the stretching frequency of the bound CO molecule (ν_{CO}) in FTIR experiments, because the nature of the distal residues has been shown to affect the ν_{CO} value in a thorough study of myoglobin mutants (37). Thus, a precise trend correlates the observed stretching frequencies to the polarity of the residues in the distal pocket. In HbIII-CO the peak frequency (1947 cm^{-1}) and the band profile are almost superimposable to those of the myoglobin mutant possessing a distal glutamine. The bandshape is broad (HWHH ~ 11 cm^{-1}) and skewed toward high frequencies and may likewise indicate the presence of more than one conformational state of bound CO. Consistently, with the presence of Gln E7, the absorption band of HbI-CO is centered at a similar frequency (1942 cm^{-1}) but is much narrower (HWHH = 3.5 cm^{-1}) and thus indicates the existence of a single conformational state of the Fe-C-O moiety. The presence of Val E10 in place of Arg in HbIII may explain these bandshape differences. The smaller Val side chain may permit alternative conformations of the nearby distal Gln E7 residue, just as in the Gln-64 myoglobin mutant in which the small Thr side chain occupies position E10 (37). The single, sharp absorption line of HbII-CO requires a more detailed comment, because it occurs at an unexpectedly high frequency (1968 cm^{-1}) despite the presence of the canonical distal histidine in position E7. In all vertebrate myoglobins and hemoglobins possessing a distal histidine, the CO stretching frequency is in the range 1940–1955 cm^{-1}, a value that has been correlated to the presence of a strong polar interaction, *i.e.* a hydrogen bond, between the His N_ϵ atom and the bound CO molecule. In turn, ν_{CO} frequencies higher than 1960 cm^{-1} are indicative of a conformational substate of bound CO with no hydrogen bonding to the carbonyl oxygen; this conformational substate in myoglobin is referred to as "A_0 conformer" (38, 39) and is little populated (~ 5%). It follows that in HbII the orientation of the distal histidine and hence its role in ligand binding may differ from the canonical one. The stabilization of an A_0-like conformer in HbII-CO may originate from a steric effect due to the methionine residue in position CD4. In fact, in SW-Mb mutants carrying a substitution of Phe CD4 with aliphatic residues, the bound CO peak is shifted to 1967 cm^{-1} (37).

In the set of myoglobin mutants studied by Li *et al.* (37) the increase of ν_{CO} was found to correlate directly with the rates of CO binding and release. The correlation holds also for the hemoglobins from *M. glutinosa* at least for the CO combination reaction. Thus, HbII is characterized by a higher ν_{CO} value relative to HbI and HbIII and by a higher rate of CO binding (Table I). The oxygen affinity of the isolated hemoglobin components does not follow the same trend. HbIII displays a 2-fold lower oxygen affinity than HbII and HbI, an effect that is almost entirely taken into account by the 2-fold lower rate of oxygen release measured in kinetic experiments at neutral pH values (Fig. 4 and Table I).

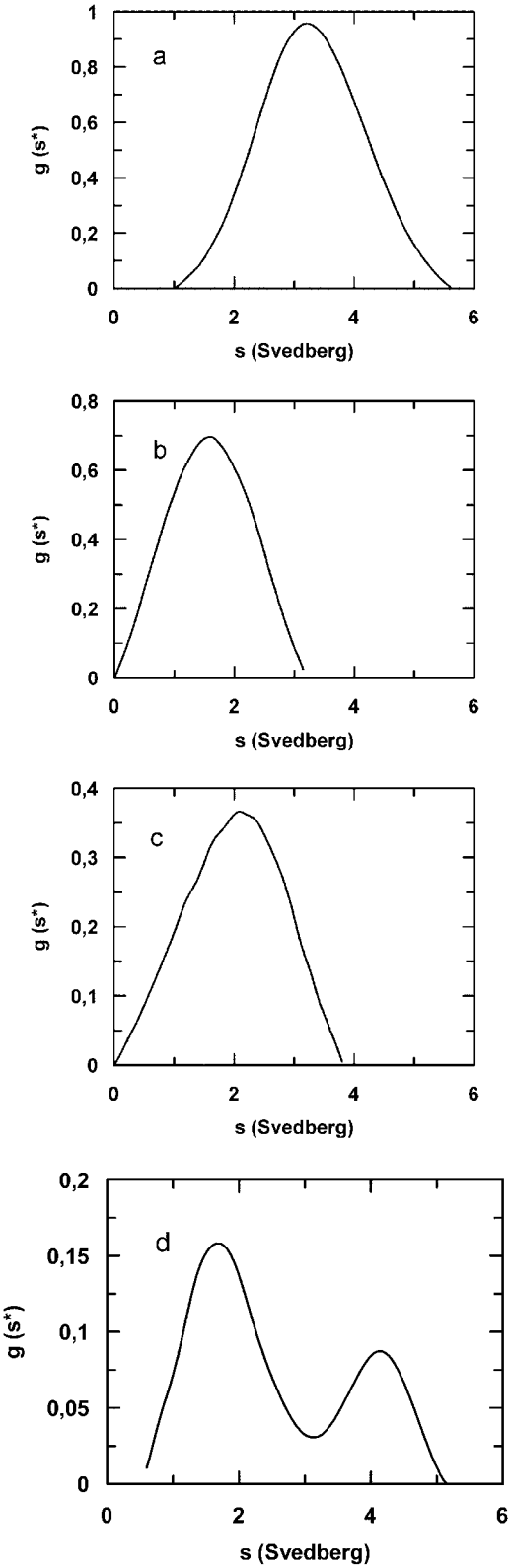

FIG. 7. **Sedimentation coefficient distribution g(s*), of binary equimolar mixtures of deoxygenated *M. glutinosa* hemoglobins.** *a*, HbI+HbII; *b*, HbI+HbIII; *c*, HbII+HbIII; *d*, total hemolysate. The protein concentration was 200 (*a* and *c*), 250 (*b*), and 60 (*d*) μM (heme) in 200 mM HEPES buffer pH 6.0 (*c*) or 7.4 (*a*, *b*, and *d*) in the presence of 10 mM $NaHCO_3$.

The most interesting properties of the hemoglobins from *M.*

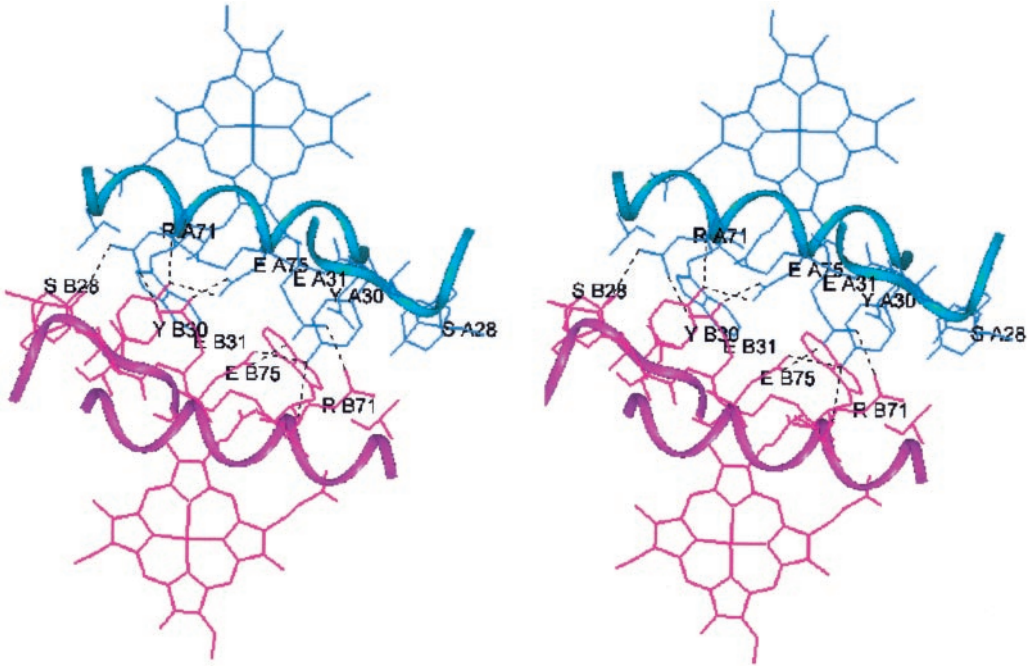

FIG. 8. **Interface residues and hydrogen bonding network in deoxygenated dimeric *P. marinus* HbV.** The coordinates of the X-ray structure (12) are from the Protein Data Bank (number 3LHB).

glutinosa concern the oxygen-linked association-dissociation phenomena, because they have distinctive features relative to the hemoglobins from lampreys. The hemoglobins from both cyclostomes associate to form dimers and tetramers in the deoxygenated state and dissociate into monomers upon ligation. In turn, the association-dissociation equilibria provide the structural basis for cooperativity in oxygen binding and for allosteric effects. In *P. marinus*, the six hemoglobin components undergo a complex pattern of homo- and heterodimer and tetramer formation (40). In *M. glutinosa*, hemoglobins are able to form homo- and hetero-oligomers, although not all the combinations are allowed. Only HbII is able to self-associate and to combine with both HbI and HbIII, as shown by ultracentrifugation (Table II) and oxygen equilibrium experiments (Figs. 4 and 5). HbI and HbIII do not interact with themselves nor with each other.

The requirement of HbII in the formation of *M. glutinosa* oligomers is intriguing. A possible explanation can be proposed on the basis of the crystal structure of deoxygenated, dimeric *P. marinus* HbV (12) and of the self-association properties of the mutant proteins constructed by Qiu *et al.* (41). In the deoxygenated lamprey hemoglobin dimer the contact area at the interface is rather restricted, 478 Å^2 (Fig. 8). It is formed by four residues from the AB corner and five residues from the E helix of each subunit and is stabilized by a network of bidentate hydrogen bonds (involving the side chains of Tyr-30, Glu-31, Arg-71, and Glu-75 and the main-chain carbonyl of Ser-28) and by the van der Waals interactions between the side chains of Trp-72 and Asn-79. Asn-79 also makes two intra-chain hydrogen bonds, one with the backbone oxygen of Glu-75 and the other with the OH group of Tyr-27. In *M. glutinosa* HbII, if one disregards Ser-28, all the interface residues are conserved with the exception of Asn-79, which is replaced by a glutamine residue. The interface of the deoxygenated HbII dimer, therefore, is likely to be very similar to that of *P. marinus* HbV. The decreased tendency to dimerize of HbII relative to lamprey hemoglobin ($K_{1,2}$ 1.7 × 10^2 *versus* 6.3 × 10^5 M^{-1} (41)) can be accounted for by the Asn-79 → Gln substitution coupled to the replacement of Tyr-27 by a methionine residue. It is relevant in this connection that the N79D and N79H mutants of *P. marinus* HbV are unable to polymerize (41).

In *M. glutinosa* HbI and HbIII, the changes at interface residues are more extensive than in HbII (Fig. 2). The substitution Tyr-30 → Phe in itself is sufficient to inhibit dimerization in recombinant lamprey hemoglobin, because it disrupts the interface hydrogen bonding network (41). The presence of Lys-71 in place of arginine in both HbI and HbIII and of Ser-75 in place of glutamic acid in HbI can likewise have a destabilizing effect on the dimeric assemblage. In HbIII a further negative contribution to the stability of the dimeric structure may arise from the presence of a leucine in place of the bulkier Trp-72. Lastly, a glutamine residue replaces the distal histidine 73 (E7) in both HbI and HbIII. In recombinant lamprey hemoglobin, this replacement inhibits self-association at neutral and slightly acidic pH values, providing an elegant proof that the structural changes accompanying dimer formation are not restricted to the interface (41).

Despite their inability to self-associate, HbI and HbIII form hybrid oligomers with HbII. The dimeric assemblage of these hybrids can be assumed to resemble that of *P. marinus* HbV and of HbII. On this basis, the presence of Tyr-30, Arg-71, Trp-72, His-73, and Glu-75 in only one of the two subunits appears to permit dimer formation. There is no information on the possible arrangement of the tetrameric assemblage.

Formation of the different hybrids has distinctive features. Thus, HbII and HbIII give rise to hybrid dimers only at pH 6.0 in the presence of bicarbonate, whereas the interaction between HbII and HbI proceeds to the tetramer stage and takes place independently of pH and of bicarbonate (Table II). In both systems polymerization of the deoxygenated protein provides the basis for cooperative oxygen binding and for the allosteric effects of protons and bicarbonate as shown by the oxygen binding data presented in Fig. 5. Thus, in the HbII-HbIII mixture, a slight cooperativity and a Bohr effect are observed only in the presence of bicarbonate. In the HbII-HbI mixture a Bohr effect is operative even in the absence of bicarbonate; the anion decreases the oxygen affinity at all pH values. The HbI-HbIII mixture, which does not polymerize, lacks cooperativity and allosteric effects.

At this point of the discussion, it is tempting to speculate on

the nature of the groups involved in the oxygen-linked binding of protons and of bicarbonate. In lamprey HbV the Bohr effect is due to an unusual cluster of four glutamyl residues formed at the dimer interface by the side chains of Glu-31 and Glu-75 of both subunits (12). The vicinity of these residues in the deoxy state raises their pK_a values from 4.5 to 6.0 and enables them to share a Bohr proton (41). In lamprey hemoglobin, bicarbonate does not behave as an allosteric effector (22). In HbII, the presence of both Glu-31 and Glu-75 is consistent with the existence of a Bohr effect. Moreover, there is no oxygen-linked binding of bicarbonate as in lamprey HbV, again in accordance with the similarity of the residues at the dimer interface. The same cluster of four negatively charged glutamyl residues can be surmised to play a central role in the Bohr effect displayed by the hybrids. In the HbII-HbIII dimers, the Bohr effect depends on the presence of bicarbonate, although the cluster of glutamyl residues is conserved. It may be envisaged that the replacement of Arg-71 with the smaller lysine residue in HbIII coupled to the presence of a methionine residue in place of Tyr-27 in HbII creates a cavity and hence destabilizes the interface unless bicarbonate is bound as a bridging ligand. In the HbI-HbII tetramers, if one assumes that the dimer provides their building block, the Bohr effect would have the same structural basis, although in HbI Glu-75 is replaced by a serine residue. In turn, the presence of Lys-71 in HbI would allow the binding of bicarbonate. It is of interest that oxygen-linked binding of bicarbonate takes place exclusively in the hybrids but not in HbII, which binds only protons in an oxygen-linked manner. This difference may depend on the smaller number of bidentate hydrogen bonds at the hybrid interface, which endows it with a larger conformational plasticity.

The physiological relevance of hybrid formation is indicated by the large effect of pH and CO_2 observed in the hemolysate (15, 21) and in whole blood of *M. glutinosa* (19, 20). In the hemolysate, the ratio between HbI, HbII, and HbIII (15:50:35) is such that mostly hybrid molecules are formed upon deoxygenation (Fig. 7*d*). Functional interactions between four different monomeric hemoglobins take place also in another hagfish species, *Eptatretus burgeri* (42) and may represent a common, distinctive feature of the hemoglobins from these primitive craniates.

In conclusion, the oxygen-linked interactions between different hemoglobin components as the structural basis for homo- and heterotropic effects can be regarded as the first attempt in vertebrates to regulate oxygen affinity through the association between different polypeptide chains.

Acknowledgments—We want to thank Prof. Peter Roepstorff from South Denmark University, Odense, for measuring the mass spectra; Winnie Heidemann, Anny Bang and Sonja Kornerup (*Myxine* banden) from Aarhus University for technical assistance.

REFERENCES

1. Perutz, M. F. (1970) *Nature* **228,** 726–739
2. Baldwin, J., and Chothia, C. (1979) *J. Mol. Biol.* **129,** 175–220
3. Antonini, E., Bucci, E., Fronticelli, C., Wyman, J., and Rossi-Fanelli, A. (1965) *J. Mol. Biol.* **12,** 375–384
4. Kellett, G. L., and Gutfreund, H. (1970) *Nature* **227,** 921–926
5. Ackers, G. K., Johnson, M. L., Mills, F. C., and Ip, S. H. (1976) *Biochem. Biophys. Res. Commun.* **69,** 135–142
6. Chiancone, E., Vecchini, P., Verzili, D., Ascoli, F., and Antonini, E. (1981) *J. Mol. Biol.* **152,** 577–592
7. Royer, W. E., Jr., Hendrickson, W. A., and Chiancone, E. (1989) *J. Biol. Chem.* **264,** 21052–21061
8. Martini, F. H. (1998) *Sci. Am.* **279,** 44–49
9. Briehl, R. W. (1963) *J. Biol. Chem.* **238,** 2361–2366
10. Goodman, M. (1981) *J. Mol. Evol.* **17,** 114–120
11. Brittain, T. (1991) *Comp. Biochem. Physiol.* **99B,**731–740
12. Heaslet, H. A., and Royer, W. E., Jr. (1999) *Structure* **7,** 517–526
13. Ohno, S., and Morrison, M. (1966) *Science* **154,** 1034–1035
14. Li, S.-L., Tomita, S., and Riggs, A. (1972) *Biochim. Biophys. Acta* **278,** 344–354
15. Fago, A., and Weber, R. E. (1995) *Biochim. Biophys. Acta* **1249,** 109–115
16. Fago, A., Malte, H., and Dohn, N. (1999) *Respir. Physiol.* **115,** 309–315
17. Ellory, J. C., Wolowyk, M. W., and Young, J. D. (1987) *J. Exp. Biol.* **129,** 377–383
18. Peters, T., and Gros, G. (1998) in *The Biology of Hagfishes* (Joergensen, J. M., Lomholt, J. P., Weber, R. E., and Malte, H., eds) pp. 307–320, Chapman and Hall, London
19. Wells, R. M. G., Forster, M. E., Davison, W., Taylor, H. H., Davie, P. S., and Satchell, G. H. (1986) *J. Exp. Biol.* **123,** 43–53
20. Perry, S. F., Fritsche, R., and Thomas, S. (1993) *J. Exp. Biol.* **183,** 165–184
21. Bauer, C., Engels, U., and Paleus, S. (1975) *Nature* **256,** 66–68
22. Nikinmaa, M., and Weber, R. E. (1993) in *The Vertebrate Gas Transport Cascade: Adaptations to Environment and Mode of Life* (Bicudo, J. E. P. W., ed) pp. 179–187, CRC Press, Boca Raton, FL
23. Paleus, S., Vesterberg, O., and Liljeqvist, G. (1971) *Comp. Biochem. Physiol.* **39B,** 551–557
24. Liljeqvist, G., Paleus, S., and Braunitzer, G. (1982) *J. Mol. Evol.* **18,** 102–108
25. Rossi Fanelli, A., and Antonini, E. (1958) *Arch. Biochem. Biophys.* **77,** 478–481
26. Friedman, M., Krull, L. H., and Kavins, J. F. (1970) *J. Biol. Chem.* **245,** 3868–3871
27. Gross, E., and Witkop, B. (1961) *J. Am. Chem. Soc.* **83,** 1510
28. Landon (1977) *Methods Enzymol.* **47,** 145–149
29. Kussmann, M., Nordhoff, E., Rahbek-Nielsen, H., Haebel, S., Larsen, M. R., Jakobsen, L., Gobom, J., Mirgorodskaya, E., Kristensen, A. K., Palm, L., and Roepstorff, P. (1997) *J. Mass Spectrom.* **32,** 593–601
30. Thompson, J. D., Higgins, D. G., and Gibson, T. J. (1994) *Nucleic Acids Res.* **22,** 4673–4680
31. Altschul, S. F., Madden, T. L., Schaffer, A. A., Zhang, J., Zhang, Z., Miller, W., and Lipman, D. J. (1997) *Nucleic Acids Res.* **25,** 3389–3402
32. Stafford, W. F. (1992) *Anal. Biochem.* **203,** 295–301
33. Johnson, M., Correia, J. J., Yphantis, D. A., and Halvorson, H. (1981) *Biophys. J.* **36,** 575–588
34. Randall, D. J. (1970) *Fish Physiol.* **4,** 253–292
35. Wells, R. M. G., and Weber, R. E. (1989) *Techniques in Comparative Respiratory Physiology: An Experimental Approach*, Society for Experimental Biology Series, Cambridge University Press, Cambridge
36. Olson, J. S., and Phillips, G. N., Jr. (1996) *J. Biol. Chem.* **271,** 17593–17596
37. Li, T., Quillin, M. L., Phillips, G. N., and Olson, J. S. (1994) *Biochemistry* **33,** 1433–1446
38. Maxwell, J. C., and Caughey, W. S. (1976) *Biochemistry* **15,** 388–396
39. Park, K. D., Guo, K. M., Adebodun, F., Chiu, M. L., Sligar, S. G., and Oldfield, E. (1991) *Biochemistry* **30,** 2333–2347
40. Rumen, N. M., and Love, W. E. (1963) *Acta Chem. Scand.* **17,** 222–225
41. Qiu, Y., Maillett, D. H., Knapp, J., Olson, J. S., and Riggs, A. F. (2000) *J. Biol. Chem.* **275,** 13517–13528
42. Bannai, S., Sugita, Y., and Yoneyama, Y. (1972) *J. Biol. Chem.* **247,** 505–510

Hagfish Hemoglobins: STRUCTURE, FUNCTION, AND OXYGEN-LINKED ASSOCIATION

Angela Fago, Laura Giangiacomo, Rossana D'Avino, Vito Carratore, Mario Romano, Alberto Boffi and Emilia Chiancone

J. Biol. Chem. 2001, 276:27415-27423.
doi: 10.1074/jbc.M100759200 originally published online April 9, 2001
